

Development of a protocol to obtain the composition of terrigenous detritus in marine sediments -a pilot study from International Ocean Discovery Program Expedition 361



Margit H. Simon^{a,b,c,*}, Daniel P. Babin^{c,d}, Steven L. Goldstein^{c,d}, Merry Yue Cai^c, Tanzhuo Liu^c, Xibin Han^e, Anne A. Haws^f, Matthew Johns^{c,d}, Caroline Lear^g, Sidney R. Hemming^{c,d}

^a NORCE Norwegian Research Centre, Bjerknes Centre for Climate Research, Jahnebakken 5, 5007 Bergen, Norway

^b SFF Centre for Early Sapiens Behaviour (SapienCE), University of Bergen, Post Box 7805, 5020, Bergen, Norway

^c Lamont-Doherty Earth Observatory of Columbia University, 61 Rt 9W, Palisades, New York 10964-8000, USA

^d Department of Earth and Environmental Sciences, Columbia University, New York, NY, USA

^e Key Laboratory of Submarine Geosciences, State Oceanic Administration & Second Institute of Oceanography, Ministry of Natural Resources, Hangzhou 310012, PR China

^f Department of Earth and Environmental Sciences, Boston College, Chestnut Hill, MA 02467, USA

^g School of Earth and Ocean Sciences, Cardiff University, Park Pl, Cardiff, CF10 3AT, UK

ARTICLE INFO

Editor: Michael E. Böttcher

Keywords:

Cation exchange wash
Sediment leaching protocol
Composition of detrital fraction
Limpopo River
IODP Expedition 361
Agulhas Current
Clay mineralogy
Radiogenic isotopes

ABSTRACT

The geochemical and isotopic composition of terrigenous clays from marine sediments can provide important information on the sources and pathways of sediments. International Ocean Discovery Program Expedition 361 drilled sites along the eastern margin of southern Africa that potentially provide archives of rainfall on the continent as well as dispersal in the Agulhas Current. We used standard methods to remove carbonate and ferromanganese oxides and Stokes settling to isolate the clay fractions. In comparison to most previous studies that aimed to extract the detrital signal from marine sediments, we additionally applied a cation exchange wash using CsCl as a final step in the sample preparation. The motivation behind the extra step, not frequently applied, is to remove ions that are gained on the clay surface due to adsorption of authigenic trace metals in the ocean or during the leaching procedure. Either would alter the composition of the detrital fraction if no cation exchange was applied. Moreover, using CsCl will provide an additional measure of the cation exchange capacity (CEC) of the samples.

However, no study so far has evaluated the potential and the limitations of such a targeted protocol for marine sediments. Here, we explore the effects of removing and replacing adsorbed cations on the clay surfaces with Cs⁺, conducting measurements of the chemical compositions, and radiogenic isotopes on a set of eight clay sample pairs. Both sets of samples underwent the same full leaching procedure except that one batch was treated with a final CsCl wash step. In this study, organic matter was not leached because sediments at IODP Site U1478 have relatively low organic content. However, in general, we recommend including that step in the leaching procedure.

As expected, significant portions of elements with high concentrations in seawater were replaced by Cs⁺ (2SD 2.8%) from the wash, including 75% of the sodium and approximately 25% of the calcium, 10% of the magnesium, and 8% of the potassium. Trace metals such as Sr and Nd, whose isotopes are used for provenance studies, are also found to be in lower concentrations in the samples after the exchange wash.

The exchange wash affected the radiogenic isotope compositions of the samples. Neodymium isotope ratios are slightly less radiogenic in all the washed samples. Strontium and Pb isotopes showed significant deviations to either more or less radiogenic values in different samples. The radiogenic isotopes from the CsCl-treated fractions gave more consistent correlations with each other, and we suggest this treatment offers a superior measure of provenance. Although we observed changes in the isotope ratios, the general trend in the data and hence the overall provenance interpretations remained the same. However, the chemical compositions are significantly different. We conclude that a leaching protocol including a cation exchange wash (e.g. CsCl) is useful for revealing the terrestrial fingerprint. CEC could, with further calibration efforts, be useful as a terrestrial chemical weathering proxy.

* Corresponding author at: NORCE Norwegian Research Centre, Bjerknes Centre for Climate Research, Bergen, Norway.

E-mail address: msim@norce-research.no (M.H. Simon).

<https://doi.org/10.1016/j.chemgeo.2019.119449>

Received 16 April 2019; Received in revised form 17 December 2019; Accepted 18 December 2019

Available online 20 December 2019

0009-2541/ © 2020 The Authors. Published by Elsevier B.V. This is an open access article under the CC BY license

(<http://creativecommons.org/licenses/by/4.0/>).

1. Introduction

IODP Expedition 361, with sites located along Africa's southeastern and southern margin, sought to assess secular variability in Agulhas Current properties and southern African hydroclimates (Fig. 1). To approach documenting changes in either the spatial distribution of rainfall variability or to assess the relationship between sediment sources around southern Africa and Agulhas Current flow, measurement of radiogenic isotope ratios on the clay size fraction of marine sediment was part of the research plan.

Strontium (Sr) and neodymium (Nd) isotopic variations produced by long-lived radioactive decay are well known as powerful tools for the study of provenance of silicate detritus in marine sediment cores. Rb–Sr and Sm–Nd isotopic systems, reflecting the weighted average of detrital components generated in different catchments, provide information on past events of crustal generation and thus represent a powerful means to investigate the provenance of river sediments (Allègre et al., 1996; Goldstein et al., 1984). Sediments derived from older crust have less radiogenic Nd and often more radiogenic Sr isotopes than those derived from younger crust, and a broad inverse relationship between $^{87}\text{Sr}/^{86}\text{Sr}$ and ϵNd is thus observed. Prior studies have successfully used the $^{87}\text{Sr}/^{86}\text{Sr}$ and ϵNd signatures of lithogenic fractions of terrigenous detritus to infer provenance, transport patterns and continental weathering states on the African continent during the Pleistocene and Holocene (Franzese et al., 2009; Franzese et al., 2006; Hahn et al., 2016; Jung et al., 2004; Rutberg et al., 2005; van der Lubbe et al., 2016). However, none of these studies aiming to target the

composition of the detrital fraction have applied a cation exchange wash, which highlights the need for this methodological study. Several processes may make the relationship of the geology in the source area and the ultimate end-members observed at the sedimentary sink difficult to deconvolve, including sediment recycling (e.g. Haughton et al., 1991), differential weathering (Jiménez-Espinosa et al., 2007), sediment sorting by the energy of the transport medium, and diagenetic alteration in the deposited sediments (Morad et al., 2000; Zabel et al., 1999).

Cation exchange washes (e.g. MgCl_2) are employed in the preparation of marine sediment to desorb elements from clay surfaces (Gutjahr et al., 2007; Tessier et al., 1979). Gutjahr et al. (2007) employed this method to remove clay-adsorbed ions before leaching the authigenic ferromanganese fraction which was then used for investigating the composition of bottom seawater in the North Atlantic, thus allowing the reconstruction of past water mass signatures. For the provenance work that is the goal of this project, both the adsorbed and authigenic fractions need to be removed, and we do not plan to use the dispersed ferromanganese fraction in the sediment fines for water mass proxy measurement. Thus, we decided to perform all of the leach steps as well as the clay separation before the ion exchange washing of the sample. We chose to use CsCl for the cation exchange wash because our goal is to obtain major and trace element chemistry as well as radiogenic isotopes from the clay fraction, and Mg is a major element that we would like to quantify. In contrast, Cs is a very minor element in clays and thus using it as an exchange reagent allows a robust measurement of the Mg concentration of the clays. CsCl is an adequate reagent for the

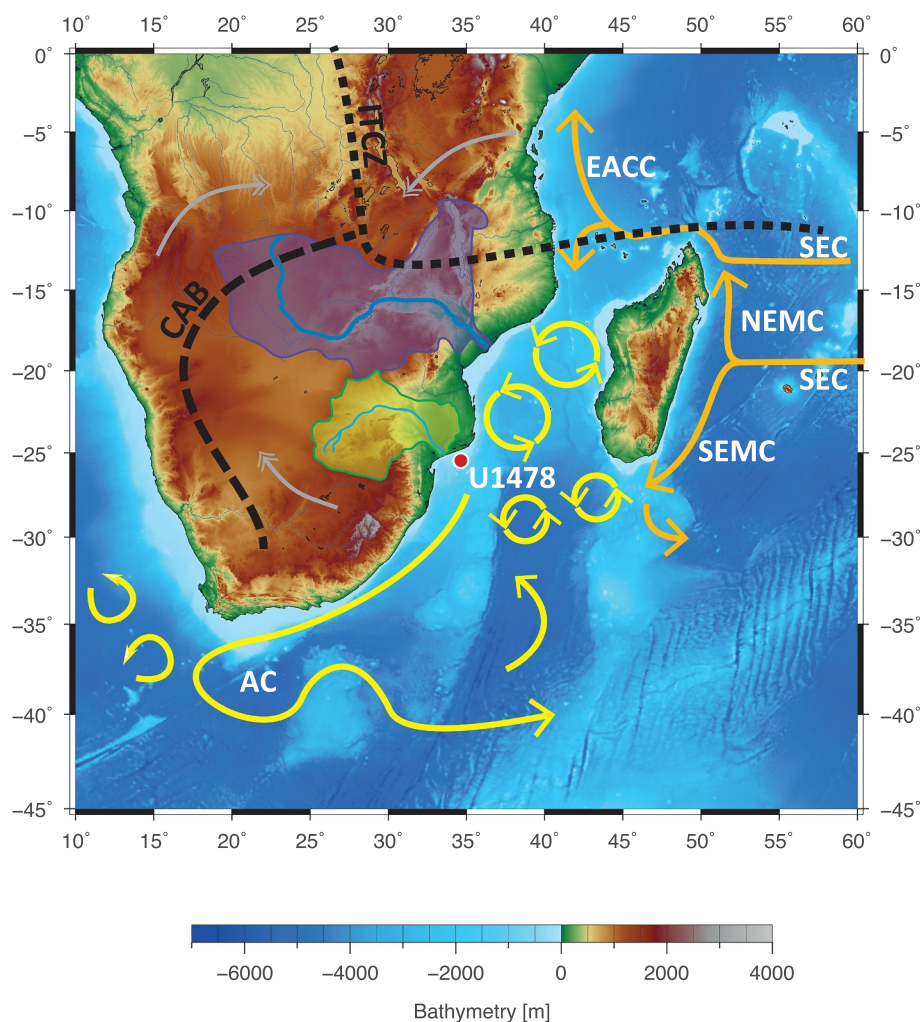


Fig. 1. Location map of IODP Site U1478 (taken from Hall et al. (2017)) with main surface currents (arrows) in the southwest Indian Ocean and atmospheric circulation over southern Africa during austral summer (December, January, February) with approximate position of the Intertropical Convergence Zone (ITCZ) and Congo Air Boundary (CAB) (dashed lines; adapted from Reason et al. (2006)). AC = Agulhas Current, SEC = South Equatorial Current, SEMC = South East Madagascar Current, NEMC = North East Madagascar Current, EACC = East Africa Coastal Current. Purple shading = Zambezi Catchment, green shading = Limpopo Catchment, gray double-headed arrows = main pathways of moisture supply to the African continent from the northwest Atlantic (through Congo) and the northwest and southwest Indian Ocean. (For interpretation of the references to colour in this figure legend, the reader is referred to the web version of this article.)

extraction of exchangeable ions as caesium has a large ionic radius but a low charge. This gives it a small hydration sphere, allowing it to form strong bonds with clay surfaces better than any other monovalent or divalent cations. Furthermore, because the Cs exchanged onto the surface will be at levels equivalent to a major element, its abundance in the exchanged clay samples will provide a measure of the concentration of ions displaced from the clay surface, as well as the cation exchange capacity (CEC) of the sample. We reasoned that the CEC of the clays may be related to their weathering history although this is not necessarily a simple relationship.

Although this is a minor procedural change, for completeness we decided to determine how the application of a cation exchange wash may impact radiogenic isotopes and other geochemical measurements, as well as clay mineralogy on the same sediment fraction during sample preparation. To our knowledge, this is the first such study to be reported. We selected samples from one of the Expedition 361 marine sediment cores in the vicinity of the Limpopo River mouth as this location receives significant detrital input from land.

2. Oceanographic, climatic, and geologic setting

IODP Site U1478 is located in the northernmost Natal Valley, on the western flank of Inharrime Terrace (25°49.26'S; 34°46.14'E), ~75 nautical miles east of the Limpopo River (Fig. 1) at a water depth of 488 m below sea level (mbsl). In this study, we show initial results from this recently drilled site, which is sensitive to local river discharge, recovered by IODP Expedition 361 in 2016 (Hall et al., 2017). The Delagoa Bight is a distinct indentation of the continental margin (Lamont et al., 2010) into which the Limpopo River, the second-largest eastward-draining river in Africa, deposits sediment. However, terrigenous material in sediments in that regime can have several potential other source areas including the Incomati, Matola, and Lusufu river catchments. Surface sediment analysis at a core site very close to Site U1478 demonstrates that the heavy mineral assemblages can be attributed to source rocks in the Limpopo catchment. However, a contribution of Matola and Lusufu end-members were also detectable (Schüürman et al., 2019).

The Delagoa Bight's hydrography is influenced by the southerly flowing waters from the Mozambique Channel and the East Madagascar Current (Lutjeharms, 2006) the confluence of which forms the Agulhas Current. The Limpopo catchment is a little over 410,000 km² and its watershed includes parts of Botswana, Zimbabwe, southern Mozambique and northern South Africa (shaded yellow; Fig. 1). The Limpopo River has a mean annual discharge of ~170 m³/s and delivers annual sediment loads of 33 Mt./y (Milliman and Meade, 1983). Its system comprises several tributaries with the most significant rivers being the Pienaars; Olifants, Serobaneng, Diep, Upper Mzingwane and Ngez.

Under modern climate, the Delagoa Bight's catchment lies in the transition between tropical and subtropical climate zones, just south of the subtropical ridge between the southern Hadley and the Ferrel cell (Tyson and Preston-Whyte, 2000). Most of the year, surface airflow is from east to west and is stronger during the summer. During winter, the South Indian Ocean anticyclone moves west and the region is under strong subsidence and anticyclonic circulation with very little rainfall. The topographic configuration of the high interior, the escarpment and the coastal lowland and the eastward propagating migratory anticyclones during the synoptic cycle create coastal shallow low-pressure cells associated with Berg winds blowing down the mountains in an offshore direction (Reason and Jury, 1990).

The Limpopo River drains the oldest terrane on the African continent. The sediment load (~35 × ~10⁶ ton/yr) is supplied by southern tributaries draining the Kaapvaal Craton (Eglington and Armstrong, 2004) and northern tributaries draining the Zimbabwe Craton (Jelsma and Dirks, 2002) as well as Karoo siliciclastic and basaltic cover. The geology of the highlands is Archean, composed of the Zimbabwe and

Kaapvaal Cratons joined by the Limpopo Belt. Bedrock in the cratons, emplaced as early as 3.8 Ga, is characteristically tonalite-trondhjemite-granodiorite, an intermediate, phaneritic, intrusive igneous rock rich in plagioclase and mafic minerals (Kreissig et al., 2000). The Limpopo Belt is a greenstone belt, composed of amphibolite-granulite grade metasediments formed between 2.9 and 2.7 by the collision of the Zimbabwe and Kaapvaal Cratons, the root of a neoArchean orogenic complex (Kreissig et al., 2000). The isotopic chemical composition of the Limpopo River catchment is distinct in that the highest ⁸⁷Sr/⁸⁶Sr signatures (between 0.73 and 0.80) and most negative εNd ratios (between -26 and -31) are yielded by muds of Limpopo tributaries draining the Kaapvaal and Zimbabwe Cratons. In contrast, Limpopo mud itself has much lower ⁸⁷Sr/⁸⁶Sr, less negative εNd, and a younger (Paleoproterozoic) age than its cratonic tributaries, suggesting more significant contributions from Karoo basalts. Additionally, material from its Pienaars tributary suggests a Paleoproterozoic age, also reflecting contributions from the Karoo Supergroup (Garzanti et al., 2014). We note that Sr isotope ratios are affected by grain size and that the study conducted by Garzanti et al. (2014) used a higher size fraction (<32 μm fraction) than targeted here.

3. Methods

3.1. Sediment leach

The detailed laboratory protocol can be found in the research method journal MethodsX. Eight samples were selected from sedimentary depths between 198 and 214 m core depth, which approximately, spans the time interval 2.4–2.8 Ma (Hall et al., 2017). In general, the effects of sediment diagenesis under methanogenic conditions in the anoxic zone of the sedimentary column should be considered when sampling to analyse the authigenic phases of marine sediments. This is crucial to consider as, within the methanogenic zone of the sedimentary column, which is anoxic, the originally present authigenic Fe–Mn oxyhydroxides are expected to be at least partially and likely completely removed or altered into other diagenetic mineral phases such as pyrite. Hence the authigenic phases still present in these sediments will have quite different chemical properties and reactivities than sediments in, for example, the sulphate-bearing zone of the sedimentary column.

The samples were sieved to separate the >63 μm fraction, to save foraminifera for further analyses. The bulk fine sediment (<63 μm), (1.7–2.1 g material per sample) was decarbonated using 1 M buffered acetic acid solution following the procedure outlined in Gutjahr et al. (2007). This step was repeated 1–3 times until once beyond the application where the sediment no longer appeared to react with the acid. Following carbonate removal the Fe–Mn oxyhydroxide coatings were dissolved by leaching the samples for 24 h, with agitation on a rocker table, at room temperature in a 0.05 M hydroxylamine hydrochloride (HH)–15% distilled acetic acid solution, buffered to pH 4 with analytical grade NaOH. The HH leaching was followed by centrifugation and triple rinses in deionized water. This sequence of procedures deviates from that of Gutjahr et al. (2007) who followed the initial carbonate leaching with a cation exchange step with MgCl₂ to desorb cations before leaching the dispersed Fe–Mn oxyhydroxide for authigenic Nd isotope measurements. Furthermore, we did not use the complexing reagent EDTA as originally suggested in the protocol of Gutjahr et al. (2007) during the leaching of the authigenic Fe–Mn oxyhydroxide fraction.

The separation of particles smaller than 2-μm diameter was carried out by settling in a column of water and adding 2 ml of 0.5% sodium metaphosphate (calgon) to each tube for the first 2 settling rounds. Particles are assumed to settle in the water according to Stokes Law. For the clay fraction (<2 μm) samples were settled for at least 3 h and 52 min. Settling rounds were performed until the water was clear, usually 15 to 20 iterations. Clods (that is small chunks of clay that are

stuck together so the sample can be weighed as a single grain) for the analysis of $^{40}\text{Ar}^*$ ages (Gombiner et al., 2016; Hemming et al., 2002) were created after the first settling round by pipetting approximately 300 μg of suspended sediment solution into a micro-centrifuge tube, centrifuging it at high speeds for 30 min, and then drying it in the oven at 60 °C.

After the clay separation, a Cs^+ cation exchange wash was performed on aliquots of the 8 samples using a 0.1 M CsCl solution. From here forward, this group of samples is referred to as the washed group. After centrifugation and removal of water, 10 ml of ethyl alcohol was added to the sample and vortexed to rinse away excess salt, then the samples were centrifuged, and decanted and the rinsing was repeated a second time. Following the rinsing, samples were dried in an oven at 60 °C. Subsamples for measuring $^{40}\text{Ar}^*$ were also taken from the aliquot containing CsCl after drying.

In this study, organic matter (OM) was not leached because sediments at IODP Site U1478 have relatively low organic content, varying from 0 to 1.25 wt% with an average of 0.45 wt% for the shipboard samples (Hall et al., 2017). However, we acknowledge that even in trace amounts in the clay fraction, OM could significantly impact CEC (pH-dependent). Thus we include a step to leach organic matter in the suggested laboratory protocol. However, it should be considered that in some cases, depending on the sediment properties, an organic oxidative leaching step with hydrogen peroxide (3%) would still not be sufficient to remove various organic phases. Stronger treatments for OM removal can, however, attack the clays and leach away soluble elements including the REE that would affect the trace element measurements. Hence this step might have to be adapted individually according to the setting and sediment composition.

3.2. Sediment dissolution

About 20 mg samples of homogenized and powdered material from the clay fraction were weighed and completely dissolved using a mixture of concentrated HF-HNO₃-HClO₄.

The dissolution of the sediment was conducted by pipetting 500 μl concentrated nitric acid (double-distilled 16 N HNO₃) into the sample beaker and sonicating for ~20 min to 1 h to disaggregate the material. Thereafter 200 μl of perchloric acid (optima grade) was added to the sample to remove organic matter and renewed sonication of the solution in the beakers was performed. Afterward, 600 μl of concentrated HF (optima grade) was pipetted into the sample and the beakers were heated on a hot plate at 150 °C overnight (> 12 h). After 12 h, the solution should be completely clear and have no suspended solids. In some cases, the sample had a black ring around the edge of the beaker likely resulting from undigested organic matter. These samples required the addition of further perchloric acid and heating. We performed a first evaporation step by heating the beakers uncapped on the hot plate at 200 °C. Thereafter 1 ml of 8 N HNO₃ was added to the beaker to perform the second dissolution step. Samples were heated in capped beakers at 150 °C on the hot plate for 2 or more hours to ensure full dissolution. Thereafter beakers were uncapped to perform the second evaporation and heated at 175–200 °C. The final dissolution of the samples was performed by adding 1 ml 4 N HNO₃ and heating the solution at 150 °C and occasional sonification until samples have gone into full solution.

Sediment standard from the Japanese Geologic Survey, Jlk-1 (Japanese lake sediment) was dissolved alongside the 16 unknown aliquots used in this study (Imai et al., 1996).

3.3. Major/trace element analysis

Major and trace element analyses were carried out using an Agilent Technologies quadrupole ICP-MS at the Facility for Isotope Research and Student Training at Stony Brook University. The 16 samples were measured alongside sediment standard Jlk. Major and trace elements

were measured simultaneously from solutions with 20,000 dilution. A mixture of all of the diluted samples was concocted as a drift solution to monitor and correct for instrumental drift. The pattern of measurements was blank, drift solution, unknown, unknown. Standards were measured with the pattern blank, drift solution, standard, twice each at the beginning, middle, and end of the analytical sessions. Samples were replicated over two sessions that took place within 24 h. The drift solution was also used to correct the offset between runs. Signal intensities were converted using the signal intensity from 12 measurements on Jlk and the concentrations from Imai et al. (1996). Precision is estimated by comparing sample replicates. For precision, we report the sample averaged percent standard deviation for each element (2SD). Precision for the major elements except Ca is better than 2%. The precision for trace elements reported here is better than 4%. Due to high Ca background and low sample Ca abundance, precision for that element is 12%. For one run, Ca had to be discarded. To achieve an accurate measurement of Cs, we applied the standard addition technique. We added 40 μl of a 100 ppm Cs solution (4 μg of Cs) to an aliquot of each Cs washed sample. To determine sensitivity to Cs, this was measured alongside an unspiked aliquot of that sample.

Concentrations of Cs determined using standard addition were converted to cation exchange capacities using the equation:

$$CEC = \frac{[Cs]}{\frac{M_{Cs}}{Q_{Cs}} * 10}$$

where [Cs] is the concentration of Cs in a sample, in ppm. M_{Cs}/Q_{Cs} represents the equivalent weight of a Cs atom, where M_{Cs} is the molar mass of Cs, and Q_{Cs} is the valence of Cs (+1). The 10 is a conversion factor to convert equivalent weight, usually reported in grams/equivalent, to 100 g/milliequivalent (meq). Using this equation will result in units of meq/100 g, a common unit for reporting cation exchange capacity.

3.4. Radiogenic isotope analysis

The Sr, Nd, and Pb isotopic measurements were performed at the Lamont-Doherty Earth Observatory (New York) using a ThermoScientific Neptune Plus multi-collector ICP-MS in static mode. Pb was extracted using Bio-rad AG*1-X8 resin and HBr and HCl column chromatography. Nd was extracted using Tru-Spec® resin followed by Eichrom Ln-Spec® resin and HNO₃. Sr was extracted using Eichrom Sr-Spec® resin. The total procedural blanks for Pb in hotplate digestions range from 21 to 30 pg and the blanks for Nd and Sr are negligible. The MC-ICP-MS instrumental drift is monitored by standard-sample bracketing using JNdi-1 for Nd, NBS 987 for Sr, and NBS 981 for Pb. Typically 30–70 standards and 20–30 samples are analyzed during a session and reported 2SD external errors are estimated from the reproducibility of the standards. These are 0.2 for ϵ_{Nd} and 0.000019 for $^{87}\text{Sr}/^{86}\text{Sr}$. For $^{206}\text{Pb}/^{204}\text{Pb}$ we report a standard reproducibility error of 0.001795; 0.0024297 for $^{207}\text{Pb}/^{204}\text{Pb}$ and 0.007317 for $^{208}\text{Pb}/^{204}\text{Pb}$. We collected 60 ratios for each run using 200 ppb solutions for Sr and Pb and 100 ppb solutions for Nd. Reported values are corrected to those of the international standards. Samples were corrected to the accepted value of the JNdi-1 standard of 0.512115 (Tanaka et al., 2000) for $^{143}\text{Nd}/^{144}\text{Nd}$, NBS 987 standard of 0.710248 for $^{87}\text{Sr}/^{86}\text{Sr}$ (Weis, 2006), and NBS 981 for 16.9405 for $^{206}\text{Pb}/^{204}\text{Pb}$; 15.4963 for $^{207}\text{Pb}/^{204}\text{Pb}$ and 36.7219 for $^{208}\text{Pb}/^{204}\text{Pb}$ (Abouchami and Galer, 1998). In-run mass fractionations was corrected using $^{146}\text{Nd}/^{144}\text{Nd} = 0.7219$ and $^{86}\text{Sr}/^{88}\text{Sr} = 0.1194$ Pb isotopes were doped with Tl in a proportion of Pb/Tl = 5. In-run mass fractionations were corrected using $^{205}\text{Tl}/^{203}\text{Tl}$ value of 2.388. Quality control was provided by measurements of rock standards BCR-2 and Jlk for Pb, BCR-2, Jlk and BHVO-2 for Sr, BCR-2, Jlk and BHVO-2 for Nd, all of which were repeatedly run through the entire dissolution and chemical separation procedures (Supplementary Table 4). The $^{143}\text{Nd}/^{144}\text{Nd}$ ratios of the samples are reported as ϵ_{Nd} .

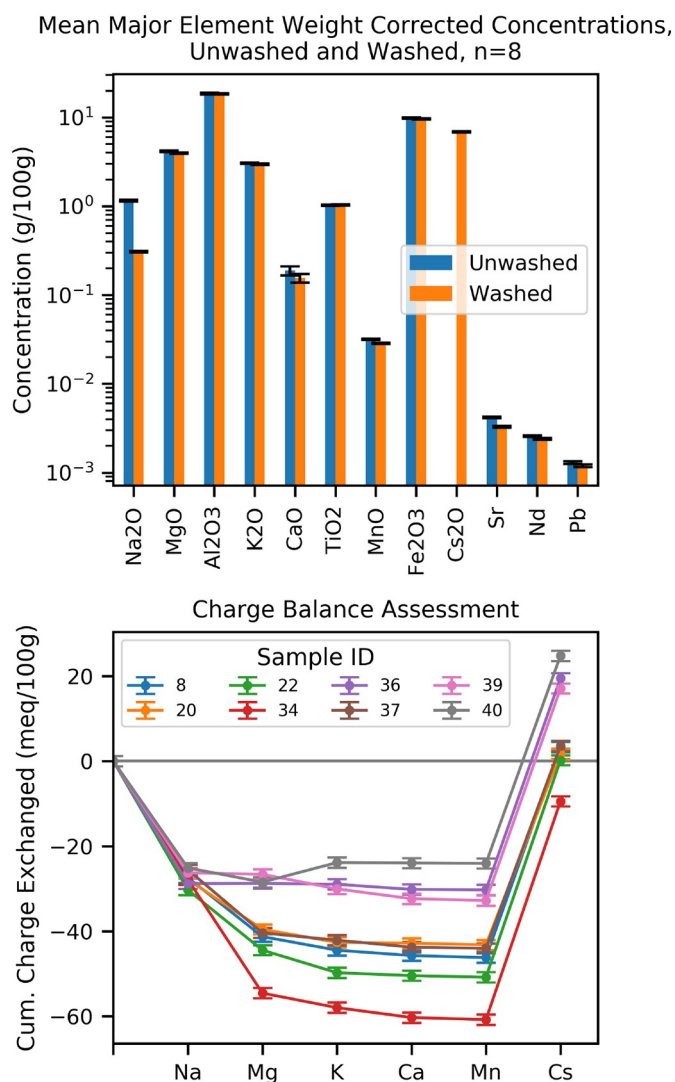


Fig. 2. A-upper panel) The magnitude of the reduction in the concentration of an element as a result of the cation exchange wash, expressed as a percent of the concentration of the unwashed group. Sample IDs are listed in Supplementary Tables 2–4 for reference. The elements bound to the clay surface in the highest relative concentrations are Na, Ca, Mn, Ba, and Sr. B-lower panel) The equivalents of cation displaced must equal the equivalents of Cs measured to conserve charge. The residual between the concentrations of the major elements in the test group (washed) and the control group (unwashed) was calculated, then converted to equivalents. Here, we visualize the summation of these charges, element-wise, for each sample. The average of all samples is plotted behind as a thick black line, with a $\pm 1\sigma$ standard deviation envelope surrounding it (light gray). Ideally, the cumulative sum of these losses should equal the equivalents of Cs. The more equivalents of Na, Mg, K, and Ca a sample lost, the higher its Cs concentration and cation exchange capacity should be.

which is the parts per 10,000 deviation of the $^{143}\text{Nd}/^{144}\text{Nd}$ value from the present-day Chondritic Uniform Reservoir (CHUR) value of 0.512638 (Jacobsen and Wasserburg, 1980).

3.5. K/Ar age analysis

Aliquots of the clay fraction were removed from the $< 2\ \mu\text{m}$ fraction of both washed and unwashed samples and dried in 1 ml micro-centrifuge tubes after the settling process. Samples were removed from micro-centrifuge tubes, weighed, and loaded into a 32-spot copper disk - typically in pairs of duplicates for 14 samples - plus 4 GLO-1 glauconite standard (Odin, 1976). To obtain a reproducible age for a

sample, we found it important to weigh and load the entire clod. Sample weights in this study ranged between 0.1 and 0.5 mg.

For each measurement session, the pattern of runs includes blanks at the beginning and end of the session bracketing the entire sequence of runs. Each air standard was bracketed by a blank measurement, and each set of 3 unknowns or GLO-1 measurements is bracketed by a blank/air/blank sequence. Signal intensities of the airs, unknowns, and GLO-1 are well above the background levels, and blank corrections are estimated from the most recently measured preceding blank. Air standards are used for quality control, to correct for any instrument drift, and to estimate the correction for the atmospheric component in the samples to yield the $^{40}\text{Ar}^*$ (that is the radiogenic argon from the decay of K in the sample). GLO-1 standards are used to quantify the sensitivity of the instrument during the session. GLO-1 has 1.109e^{-12} mol of $^{40}\text{Ar}^*$ per mg of sample (Odin, 1976). The sensitivity of the mass spectrometer/extraction line system for argon is $\sim 5.13\text{e}^{13}$ nanoamps/mol. Signals are measured on an analogue multiplier with high voltage set such that 1 nanoamp is approximately 10 mv on a $10^{11}\ \Omega$ resistor. The reproducibility of the age of GLO-1 is between 1 and 2% for most sessions (2 SD). Reproducibility of the sediment clods is not generally as good as for the GLO-1, and when the difference between aliquots is $> 10\%$, additional aliquots of the sample are repeated in another session.

3.6. Clay mineral analyses

Clay mineralogy determinations were performed under three conditions, i.e., air-drying, ethylene-glycol solvation for 24 h, and heating at $490\ \text{°C}$ for 2.5 h, by standard X-ray diffraction (XRD) on a PANalytical X'Pert Pro diffractometer in Key Laboratory of Submarine Geosciences, China, SOA with $\text{CuK}\alpha$ radiation and Nifilter, under a voltage of 45 kV and an intensity of 40 mA. Identification of clay minerals and calculation of their relative proportions were made according to the position and area of the (001) series of basal reflections on the three XRD diagrams (not shown), i.e., smectite (001) including illite/smectite mixed-layers at $17\ \text{Å}$, illite (001) at $10\ \text{Å}$, and kaolinite (001) and chlorite (002) at $7\ \text{Å}$ (Biscaye, 1965). Relative proportions of kaolinite and chlorite were determined based on the ratio from the $3.57/3.54\ \text{Å}$ peak areas. Additionally, illite crystallinity was obtained from the full width at half maximum (FWHM) of the $10\ \text{Å}$ peak (Esquevin, 1969). Semi-quantitative calculations of all the included peak parameters were performed on the glycolated curves using Jade6. Clay mineral analyses were performed on oriented mounts. Results on the washed fraction can be found in the Supplementary information.

4. Results

4.1. The effects of adsorbed cation removal and CsCl wash on clay geochemistry

4.1.1. Major and trace elements

Here we assess which elements were exchanged during the procedure as well as the effectiveness of the exchange wash. Fig. 2A depicts how the wash changes the composition of the samples via cation exchange. The differences in concentrations, including uncertainties, between washed and unwashed aliquots are shown. Note the log scale, used to accentuate changes in concentration. All of the data reported here are from samples dissolved with HF, so Si was lost. Most notable here is that by far and away, Cs is replacing Na on the clay surfaces. Sodium concentration is reduced by 75% on average. Less outstanding is the loss of other soluble major elements: Ca (22%), Mn (14%), Mg, (14%), and K (8%). Ca concentrations in the clay are extremely low ($\sim 0.12\ \text{g}/100\ \text{g}$), and tuning the quadrupole mass spectrometer to achieve precise measurements on this low abundance major element, the other major elements, and trace elements simultaneously was a challenge. Concentrations of elements predominantly integrated into

the structure of clay minerals, such as Al, Fe, and Ti, are not changed by the wash outside of the reported analytical uncertainty. Concentrations of trace metals Sr and Nd, used by geochemists as isotopic tracers, appear to decrease as a result of the exchange wash by 25%.

We test the effectiveness and quality of the exchange using a charge balance. However, this balance is not trivial because mass is not conserved in the exchange reaction. Replacing light elements like sodium with the heavier element caesium creates an appreciable weight difference between the washed and unwashed samples. So first we simulate a “mass balance” by estimating what percent of each major element is lost, on average. We determine what fraction that element contributed to the total losses by summing those percents and normalizing them to 100. For example, about 75% of Na is lost in each sample during the washing, but this represents only ~60% of total ions exchanged. To simulate this “mass balance,” we model the weight change of replacing each element (e.g. Na, 23 g/mol) with Cs (133 g/mol) at

the percent it contributed to the cations exchanged. The above calculations reveal each sample is ~5 g/100 g heavier after the exchange wash. The calculation process artificially removed this extra weight.

To complete the charge balance, we take exchangeable major element oxides (Na, Mg, K, Ca, and Mn) and convert them first to moles, and then to equivalents using their atomic charge. Ideally, the charge of the exchangeable cations lost and the charge of Cs^+ ions gained should sum to zero. Therefore, we visualize the charge balance as a cumulative sum (Fig. 2B). The bulk of the charge displacement comes from Na and Mg, as noticed previously. Of the 8 samples, 4 return to zero within error. 3 samples gained more Cs than they lost exchangeable cations. One sample does not appear to have gained enough Cs. See the discussion section for potential explanations for this apparent charge imbalance. We admit that these results are troubling, as they would cause us to question the accuracy of our Cation Exchange Capacity measurements. We believe this is a function of accumulated uncertainties,

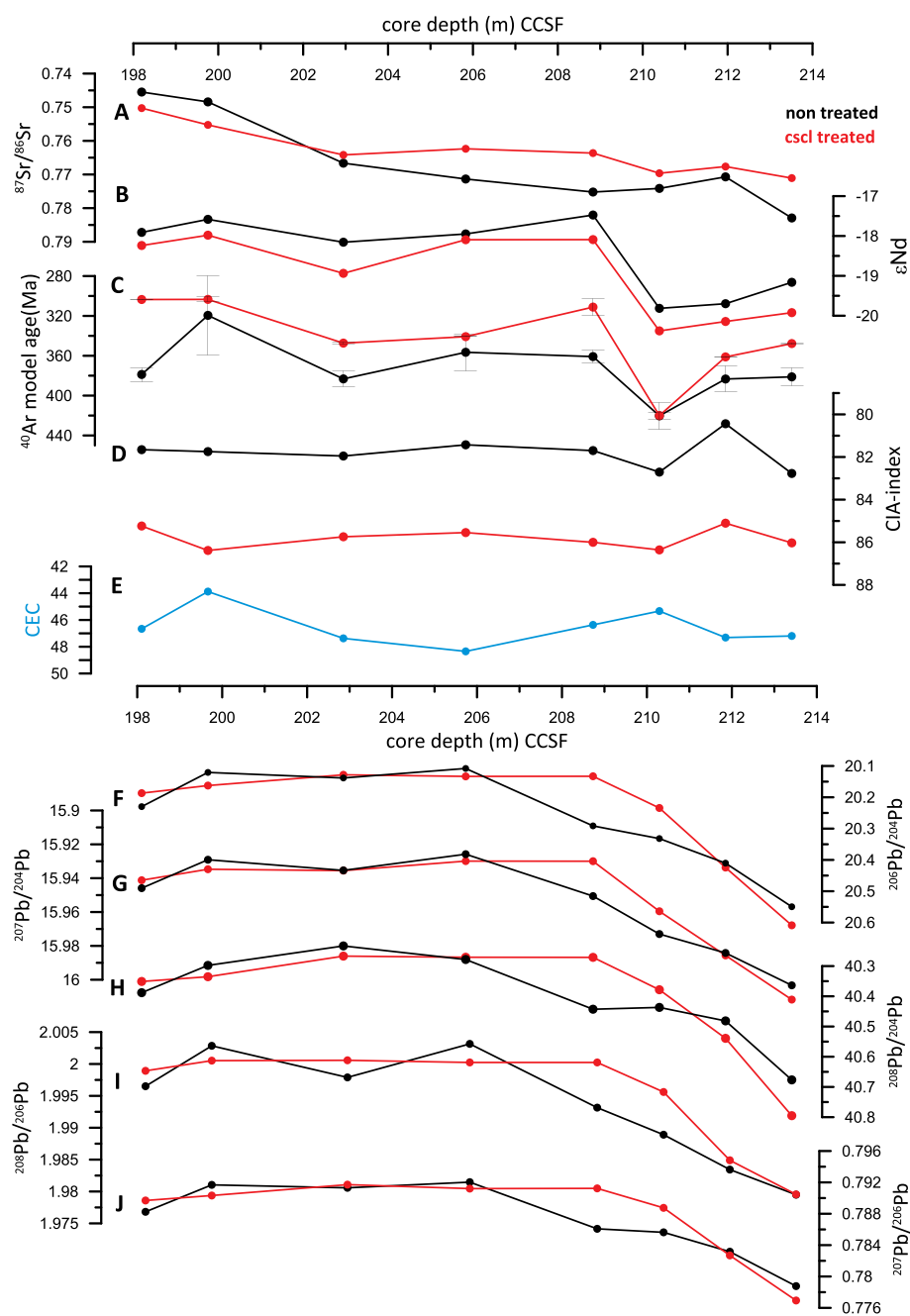


Fig. 3. Overview of relative compositions of CsCl treated and non-treated samples against core depth in m. Red displays the CsCl treated aliquot for each sample. A: Comparison for $^{87}Sr/^{86}Sr$, average ($n = 16$) $^{87}Sr/^{86}Sr$ 2 SE measurement error: 0.000012; B: ϵNd ; average ($n = 16$) 2 SE measurement error: 0.07; C: ^{40}Ar model age in Ma calculated using the 2% K, error is the ± 1 s (Ma); D: Chemical Index of Alteration (CIA, (Nesbitt and Young, 1982a)); E: Cation exchange capacity (CEC,); F: $^{206}Pb/^{204}Pb$, average ($n = 16$) 2 SE measurement error 0.0004 G: $^{207}Pb/^{204}Pb$, average ($n = 16$) 2 SE measurement error: 0.00036H: $^{208}Pb/^{204}Pb$, average ($n = 16$) 2 SE measurement error: 0.001044; I: $^{208}Pb/^{206}Pb$, average ($n = 16$) 2 SE measurement error: 0.00023; J: $^{207}Pb/^{206}Pb$, average ($n = 16$) 2 SE measurement error: 0.00010. (For interpretation of the references to colour in this figure legend, the reader is referred to the web version of this article.)

but more tests should be performed to increase the confidence in the CEC.

4.1.2. Radiogenic Isotopes

Six of 8 washed samples have $^{87}\text{Sr}/^{86}\text{Sr}$ values that are significantly lower (beyond measurement error) than their non-treated counterparts (Fig. 3A, Supplementary Table 1). Washed samples have uniformly less radiogenic ϵNd values (Fig. 3B), beyond the measurement error (Supplementary Table 1). Pb isotopes are not uniformly affected by the cation exchange wash. Four out of 8 samples have more radiogenic Pb isotopic ratios, and four out of 8 have less radiogenic Pb isotopic ratios (Fig. 3F–J). They correlate strongly with each other ($R^2 = 0.80\text{--}0.97$), but less strongly to other measures of provenance (ϵNd : $R^2 = 0.3\text{--}0.63$, $^{87}\text{Sr}/^{86}\text{Sr}$: $R^2 = 0.29\text{--}0.36$, and Ar: $R^2 = 0.034\text{--}0.34$) (not pictured).

$^{40}\text{K}/^{40}\text{Ar}$ ages from the washed samples are systematically younger than from the unwashed aliquot (Fig. 3C) and they have lower % radiogenic ^{40}Ar . Out of 8 samples 6 unwashed ones are 4–10% older than their washed counterparts. Two unwashed sample, MS22 and MS 34 yielded ages which are 15–22% older, respectively. The unwashed samples, in general, are less reproducible (Fig. 3C), and subsequently we found that because of this small-scale heterogeneity it is necessary to weigh the entire clod to get consistent results.

There are many reasons why different isotope systems used as

provenance indicators may yield different results from each other, such as the varying temperatures at which different systems close and how they are affected by diagenesis, weathering, and clay mineral formation. However, in principle, we would expect that they show some similarities, reflecting the chemistry of their source regions. Therefore, we compare trends in isotope systems and quantify these using linear regressions. We argue that if the correlation changes, it is most likely the result of authigenic phases biasing the radiogenic isotope signature.

We present a linear regression of each isotope ratio used for provenance to all the others for both the unwashed (Fig. 4A–F, left panel) and the washed group (Fig. 4A–F, right panel). The application of our procedure resulted in trends in isotopic compositions within the washed group that more resemble each other: the regressions from the washed group have higher correlation coefficients. These data demonstrate how the wash affected the composition of radiogenic Sr in our samples. Before the wash, ϵNd does not have a strong correlation with $^{87}\text{Sr}/^{86}\text{Sr}$ ($R^2 = 0.25$) (Fig. 4A). There is weak correlation between the ^{40}Ar model age and $^{40}\text{K}/^{40}\text{Ar}$ with $^{87}\text{Sr}/^{86}\text{Sr}$ ($R^2 = 0.2, 0.04$) (Fig. 4B–C). When radiogenic isotope measurements are compared among the washed group, the trends between each isotope system are more obviously systematic. The relationship of $^{87}\text{Sr}/^{86}\text{Sr}$ to ϵNd and $^{40}\text{K}/^{40}\text{Ar}$ is most improved with an R^2 improving from 0.25 to 0.6 and from 0.05 to 0.49 respectively (Fig. 4A; C).

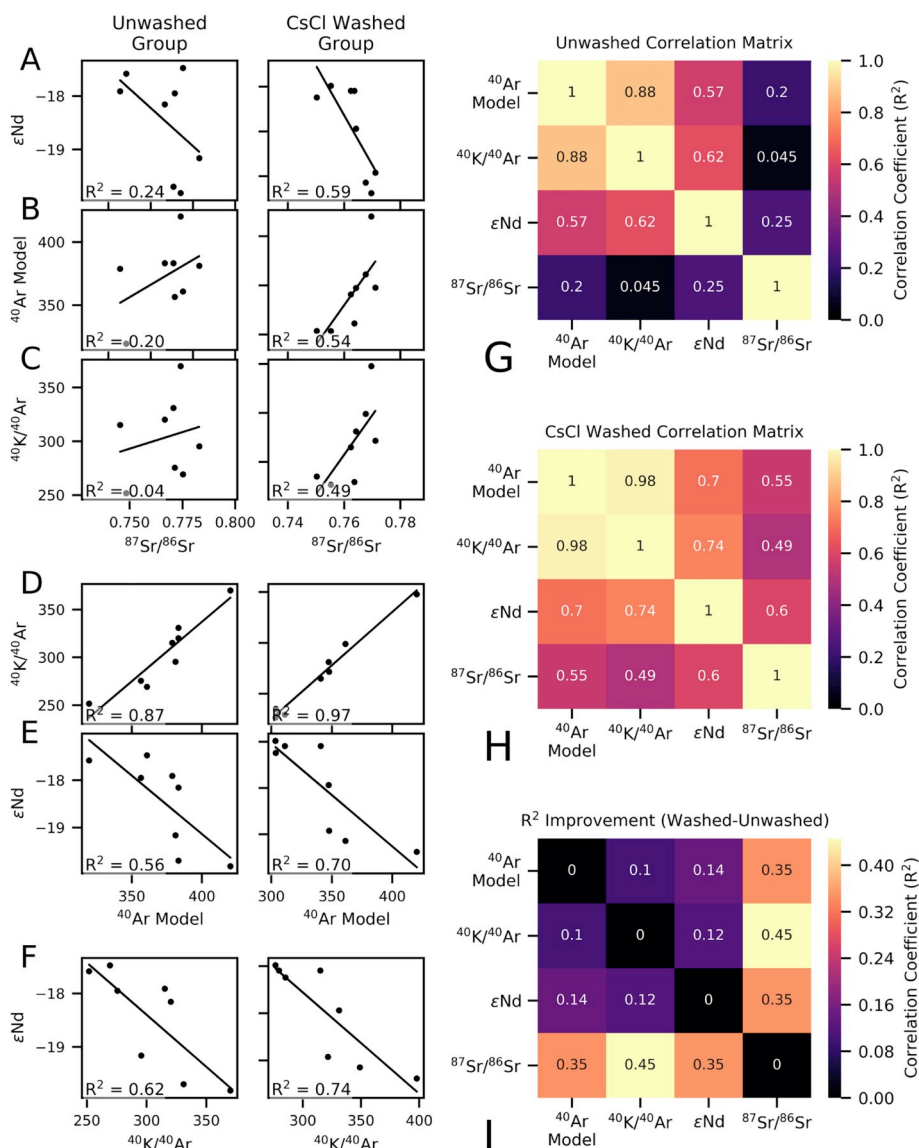


Fig. 4. Left panels show correlations between the control group (non-treated aliquots) and right panels display correlations between test groups (CsCl-washed). R^2 correlation coefficients displayed at the bottom of each plot A) Correlations of ϵNd and $^{87}\text{Sr}/^{86}\text{Sr}$ and (Ma) B) Correlations of ^{40}Ar model age (Ma) and $^{87}\text{Sr}/^{86}\text{Sr}$ C) Correlations $^{40}\text{K}/^{40}\text{Ar}$ (Ma) and $^{87}\text{Sr}/^{86}\text{Sr}$. D) Correlations of $^{40}\text{K}/^{40}\text{Ar}$ (Ma) and ^{40}Ar model age (Ma). E) Correlations of ϵNd and ^{40}Ar model age (Ma). F) Correlations of ϵNd and $^{40}\text{K}/^{40}\text{Ar}$ (Ma). (Right) Correlation matrices were generated to evaluate the effect of CsCl wash holistically. Warmer colors represent higher degrees of correlation. G) R^2 values without the CsCl wash. H) R^2 values of clays washed with CsCl. I) The effects of the procedure are better visualized by subtracting the washed (H) and unwashed (G) matrices, visualizing the difference before and after the procedure. Correlations of $^{87}\text{Sr}/^{86}\text{Sr}$ to $^{40}\text{K}/^{40}\text{Ar}$ and ϵNd are notably improved by the CsCl wash, depicted with warmer colors.

As expected, the ^{40}Ar model age, calculated assuming a uniform 2% K, correlates strongly with the $^{40}\text{K}/^{40}\text{Ar}$ age, which is calculated with the measured K ($R^2 = 0.87$). The $^{40}\text{K}/^{40}\text{Ar}$ age correlates more strongly with ϵNd than the ^{40}Ar model age (Fig. 4D, E), ($R^2 = 0.62$ vs $R^2 = 0.56$). The relationships of all of these isotopic tracer proxies are improved by the wash, but less dramatically than for Sr isotope composition.

Matrices of correlation coefficients were generated to evaluate the effects of the procedure. Fig. 4G shows the R^2 coefficients before the procedure, among the unwashed group, and Fig. 4H shows the R^2 coefficients after. The effects of the procedure are best visualized by subtracting the before (Fig. 4G) and after (Fig. 4H) matrices to generate a matrix of anomalies (Fig. 4I). Correlations of $^{87}\text{Sr}/^{86}\text{Sr}$ to $^{40}\text{K}/^{40}\text{Ar}$ and ϵNd are notably improved by the CsCl wash, with the highest anomaly and warmest colors (Fig. 4I).

4.2. Clay mineralogy

The major clay minerals in the samples were identified by X-ray diffraction techniques (Fig. 5). In general we find that illite is the most abundant, smectite is second, and kaolinite is third. Chlorite could not be detected in the 8 samples. Illite values range from 29 to 50% in the unwashed fraction and tend to increase down-core. Smectite has a range of values from 24 to 42% and showing a decreasing trend over time. Kaolinite seems to vary around a mean between 21 and 30% (Fig. 5). Further details on the clay minerals in the washed aliquot can be found in the Supplementary Information.

4.3. Chemical Index of Alteration (CIA) and Cation exchange capacity (CEC) of the clay fractions

The Chemical Index of Alteration (CIA), (Fig. 3D) estimates the extent of weathering of continental rocks and sediments, where higher values indicate greater alteration, and is very useful in the interpretation of marine sediments.

$$\text{CIA} = 100 * \text{Al}_2\text{O}_3 / (\text{Al}_2\text{O}_3 + \text{CaO} + \text{Na}_2\text{O} + \text{K}_2\text{O})$$

Cation exchange capacity (CEC) is used in agriculture as an assessment of soil fertility, indicating the capacity of the soil to retain several nutrients (e.g. K^+ , NH_4^+ , Ca^{2+}) in plant-available form. The extent of weathering of soil can be estimated from its CEC, as the availability of exchangeable cations depends on clay mineralogy, which is a function of the substrate composition and degree of chemical weathering.

We calculated the index for both sets of samples and find that the CIA based on the CsCl treated samples has higher values than the non-treated aliquots (Fig. 3D). CEC of samples has a range from 42 to 49 over the core depth covered in this study (Fig. 3E). Measurements of CEC and CIA have an inverse relationship ($R^2 = 0.47$) (Fig. 6). High measurements of CIA indicate high chemical weathering in rocks, given that aluminum remains in the weathering residue. Low CEC indicates a breakdown of primary minerals to secondary clay minerals as a consequence of weathering. Here, a lower CIA, suggesting lower chemical weathering extent, correlates negatively with higher measurements of CEC, suggesting lower degrees of secondary mineral formation.

5. Discussion

5.1. The effects of adsorbed cation removal and CsCl wash on clay geochemistry

5.1.1. Major and trace elements abundant in seawater removed by exchange wash

Our geochemical results demonstrate that Na concentrations are most affected by the CsCl rinse, reduced by 75% (Supplementary Table, Fig. 2A). This suggests that much of the material bound to the clay

surface is Na^+ ions, far and away the most abundant ion in seawater. Cs^+ replaces Na^+ , bound to the surface of the clay, during the washing procedure due to the powerful hydration sphere of the Cs^+ and the high concentration of ions available for the exchange in the 0.1 M solution. Also affected are Ca, Mg, and K concentrations, the 3rd, 5th, and 6th most abundant elements dissolved in seawater.

This change in our perception of major element chemistry has consequences. The CIA of marine sediment, dependent on concentrations of major elements, is commonly used as both a tracer and to appraise changes in weathering on the landscape (Garzanti et al., 2014). Here, our CIA measurements are higher using the Cs^+ treated value compared to the non-treated aliquots (Fig. 3D). This pattern results from the 75% reduction in the Na values in the Cs^+ washed sediment. We argue that this CIA measurement after the exchange wash provides a more realistic terrestrial signal, appraising the concentrations of only the structural components of the clay. The composition and rate of authigenic cation binding to clay minerals could depend on salinity and pH of seawater, transport pathways, and depositional environment, factors that could change on varying timescales.

We find reduced concentrations of strontium and neodymium in all samples that have undergone the Cs^+ cation exchange wash. Sr concentration in seawater is relatively high for a trace element, at ~ 10 ppm (Angino et al., 1966). The source of strontium is rocks of the continental crust delivered to the ocean in sediments, but it is highly soluble like its alkaline earth relative calcium and has a long residence time in seawater of ~ 5 Myr (Palmer and Elderfield, 1985). Nd is also sourced from the continental crust and sediments but has a much lower concentration (~ 0.1 – 0.3 ppb) and much shorter residence time (200–1000 years) (Goldstein and O'Nions, 1981; Tachikawa et al., 2003; van de Flierdt et al., 2016). We attribute the loss of these elements to the fact that seawater derived Sr and Nd that has been adsorbed on the clay's surface in the marine environment are exchanged away with the CsCl solution. The isotopic composition of this material displaced by Cs^+ ions may have the potential to bias our measurements

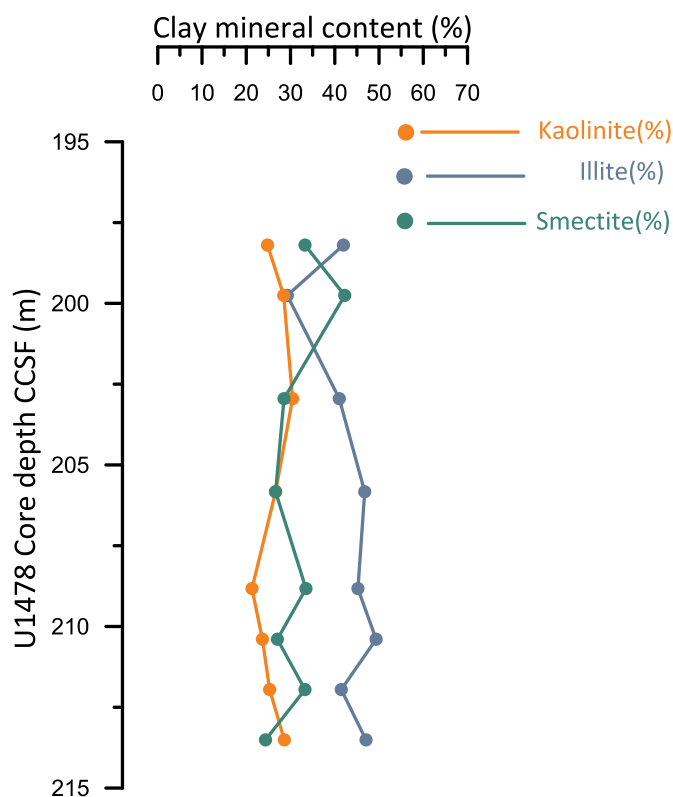


Fig. 5. Clay mineral content down core of the 8 test samples from IODP Site U1478 without CsCl treatment.

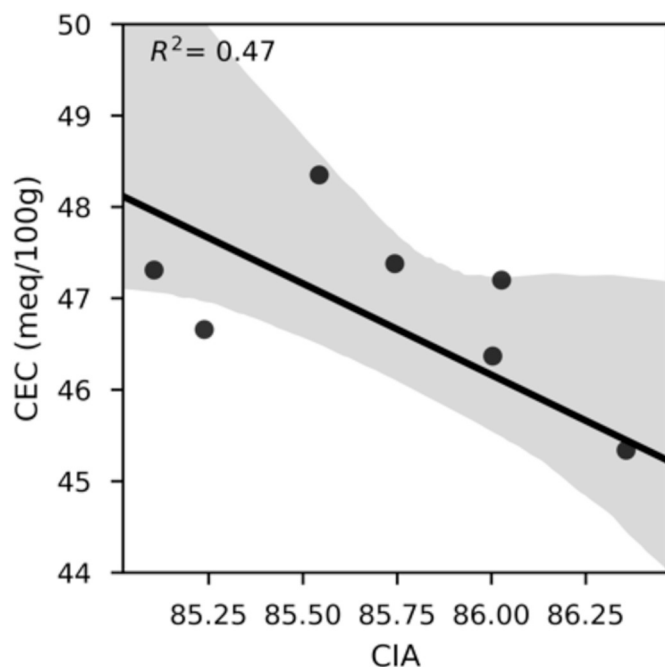


Fig. 6. Relationship between Cation Exchange Capacity (CEC) and Chemical Index of Alteration (CIA). The CEC of clay minerals relates to the Chemical Index of Alteration inversely. Lower Chemical Index of Alteration indicates less aluminum enriched material. This is often interpreted as the result of low chemical weathering, which does not flush away soluble cations. In our data, we see that samples with a low CIA tend to have higher CEC, indicating more smectite compared to illite and kaolinite, an observation that would also be consistent with lower degree of chemical weathering. Differences in the responses of the proxies to weathering processes include CIA's likely greater sensitivity to bedrock chemistry and source terrain, and CEC's potentially parabolic response to landscape residence time and soil flushing.

if not accounted for or removed.

How and when are cations usually adsorbed onto the surface of the clay? Studies have shown that diagenesis of clay minerals may occur when they are transferred from freshwater to seawater via the river system. The mechanism involves reactions of the cations and anions in seawater with the minerals through exchange, whereby a rearrangement of the cations in the exchange positions takes place (Carroll and Starkey, 2013).

Accounting for the conservation of charge in our data was a challenge: 4 of the 8 samples failed to achieve balance from the exchange. 3 samples appeared to collect more Cs than equivalents of soluble major elements were displaced, a positive balance. We offer a likely explanation for this set: organic matter in the finest fraction may have absorbed additional Cs in a way that we did not account for. This yields an important takeaway: given the very high cation exchange capacity of organic matter, it could contribute to CEC significantly even with relatively low concentrations of organic matter in bulk sediment. Therefore, we advise a step to oxidize organic matter to be introduced before the cation exchange wash.

Other problems contributing to the imbalance may be rooted in 1) analytical uncertainty in major elements and/or Cs leading to an accumulated error larger than we thought. Ca concentrations were difficult to measure because of its low concentration but Ca did not contribute to the charge balance enough to explain the observed imbalance. 2) the partial dissolution of clay minerals during the cation wash, limiting the ability of the clay to hold charge, contributing to a negative balance. This is also highly unlikely given the reagent was a low concentration (0.1 N) salt solution, with a pH of 4.5. More work would be needed to fully evaluate the charge balance.

5.1.2. Effects on radiogenic isotopes

The cation exchange wash may improve the fidelity of the radiogenic isotope proxies. Our logic is that if the different provenance proxies correlate more strongly with one another after the wash, that regression line must be pointing more accurately towards the isotopic composition of the source, or mixing sources.

The present-day seawater $^{87}\text{Sr}/^{86}\text{Sr}$ is 0.70918 (Henderson et al., 1994). In this study, we find $^{87}\text{Sr}/^{86}\text{Sr}$ between 0.74 and 0.77 (Supplementary Table), which points to a continental detritus origin of the signal. Two out of six samples treated with the Cs^+ wash yield more radiogenic ratios than before the treatment (beyond the measurement error of 0.00001), which could be explained by the removal of seawater derived Sr from the clay surface, thus altering the ratio towards more radiogenic values (Fig. 3A). Conversely, the remaining samples show the opposite $^{87}\text{Sr}/^{86}\text{Sr}$ trend, which cannot be explained by the removal of seawater derived Sr. However, in all cases, the removal of adsorbed Sr, whatever its isotopic composition, reveals $^{87}\text{Sr}/^{86}\text{Sr}$ values that correlate better with other isotopic measurements on the sample, as the CsCl wash improved correlations of Sr isotopes with other source-based proxies (ϵNd and $^{40}\text{K}/^{40}\text{Ar}$ age) (Fig. 4). Because of these improvements, the application of the cation wash is recommended for provenance studies employing Sr isotopes on clay minerals. While the observed magnitude of change on $^{87}\text{Sr}/^{86}\text{Sr}$ ratios from the CsCl washed aliquots is large (0.0025–0.08), and the correlations with the other isotopes are better, the overall trends in the correlations are the same, indicating that the general provenance interpretations of studies lacking a cation exchange wash are nevertheless valid.

All Cs^+ -treated samples yield less radiogenic ϵNd values compared to their counterparts of 0.2–0.7 ϵNd units. The offsets are beyond the analytical uncertainty of the measurement (error (2SD): 0.2 ϵNd units for the set of 16 samples), (Supplementary Table 1). Neodymium isotope ratios at ~500 m depth near our core site 1478 are ~ -12 (Jones, 2010). Exchanging away seawater authigenic Nd from the clay's surface would shift ϵNd values towards less radiogenic values as seen in our results. This would suggest that by applying a Cs^+ treatment the final ϵNd represents a purer detrital sediment signal overall. The removal of reabsorbed Nd from authigenic phases in seawater and the improved detrital signal of the sediment is also confirmed by the correlations (Fig. 4). All sample values become systematically less radiogenic however, the magnitude of this shift is small compared to potential shifts caused by a change in provenance.

For the five measured Pb isotope ratios, we cannot find any systematic offset, which makes it difficult to directly infer whether the wash leads to a more robust detrital signal. It could, however, also be governed by the fact that Pb, due to its low solubility, does not travel very far in seawater, possibly resulting in fairly similar compositions between authigenic and terrigenous phases.

Comparing the average ϵNd and $^{87}\text{Sr}/^{86}\text{Sr}$ values from our data set to the published values from the Limpopo catchment area indicates a good match within the reported range by Garzanti et al. (2014), which confirms the Limpopo system source of this detrital fraction. Minor deviations might be related to different grain size fractions measured in both studies and the applied sediment leaching techniques. The washed population with slightly less radiogenic average ϵNd values would indicate an even better match with the terrestrial dataset compared to the unwashed ones. We avoid making an attempt to interpret changes in sources through time based on our very limited dataset: only 8 samples spaced over ~10 m of core.

We find that the $^{40}\text{K}/^{40}\text{Ar}$ age of washed samples tend to be younger than the unwashed samples. We suggest this is the result of grain size and density effect in the process of creating the small clods (sample weights are 0.1–0.5 mg for the $^{40}\text{Ar}^*$ measurements). Unwashed clods appear thin, glossy, and have a dark colour. Replicate analyses on these clods consistently yield higher standard deviations than in the washed aliquot. Additionally, it appears older ages could result from a tendency to sample the densest parts of the clod, near the center of the

microcentrifuge tube. In the washed clods, it does not appear to matter which part is sampled for analyses. Among clay minerals, illite is the only significant K-bearing one. It is also denser (2.6–2.9 specific gravity) than minerals from the smectite group (montmorillonite = 1.7–2.0). Thus, in dried unwashed samples, the center of the clod might contain the oldest, densest clay minerals. In dried, Cs washed aliquots however, selecting different parts of the sample yielded the same $^{40}\text{Ar}^*$ concentrations. Clay flocculates more readily in the Cs ion rich solution of the washed samples, causing them to settle more quickly and uniformly, and thus reducing the sorting effect and providing a more homogenized $^{40}\text{Ar}^*$ measurement. Experimentation confirmed this in the unwashed aliquot, and this effect can be mostly corrected for by weighing and measuring the entire sample clod.

We conclude our discussion by restating our inference that the exchange wash has the effect of improving correlations between isotopic measurements on a set of samples because the removed adsorbed cations obscure the true, terrigenous signal endemic to the clays of the sample. Variations in local dissolved seawater cations, the aqueous geochemistry of the river catchment, changes in salinity or pH of seawater, transport processes and duration, and landscape storage are among the list of many potential factors that could affect the chemical composition of cations bound to clay minerals. These might have the effect of biasing that terrestrial signal.

5.2. Potential additional indicators of environmental information: the application of the Chemical Index of Alteration (CIA) and Cation exchange capacity (CEC) of the clay fractions

Positively-charged ions are adsorbed to soil surfaces by the electrostatic interaction between their positive charge and the negative charge of the surface (Schaetzl and Thompson, 2015). Exchangeable cations thus form part of the diffuse layer above the charged surface. These cations can easily be displaced from the surface by other cations from a surrounding solution, as the binding is relatively weak. Cation-exchange capacity is measured by displacing all the bound cations with a concentrated solution of another cation, and then measuring either the displaced cations in solution or the amount of added cation that is retained on the solid (Bache, 1976). In this study, we used a CsCl solution because Cs^+ is a trace element in the natural solids and thus its concentration in the washed sample is a potential measure of the CEC.

CIA and CEC have an inverse relationship and are moderately correlated (Fig. 6). However, a poor correlation might be expected because the proxies are not sensitive to exactly the same processes. CIA was designed to quantify degree of bedrock weathering, and thus would be sensitive to sediment source sorting processes. A study from Changjiang River basin, China has questioned whether the CIA reflects silicate weathering, and concluded that it probably indicates the integrated weathering history in the river basin, and thus, cannot be used as a reliable proxy of instantaneous chemical weathering (Shao and Yang, 2012). Furthermore, the hydrodynamic sorting also influences the CIA values. On the other hand, the CEC may be sensitive to the climate of the clay minerals' formation, and the residence time of the sediment on the landscape. In one endmember scenario, extremely high rates of physical weathering and erosion could result in the deposition of primary minerals with low CEC, such as the glacial flour in Owens Lake (Bischoff et al., 1997). In another endmember scenario, low rates of erosion coupled with high soil flushing could produce laterite soils, rich in Fe and Al oxides, which would also have extremely low CEC.

This study shows that a CsCl exchange wash can be applied to marine sediments (sensitive to terrestrial input from land) to derive the cation exchange capacity in clay minerals. The CEC measurement gave a qualitative prediction of the clay mineralogy of the sample, as the proportion of kaolinite to smectite appeared to control CEC. Because clay mineralogy relates to terrestrial weathering processes, there is a potential for CEC to indicate climate conditions and chemical weathering extent. In our data, the CEC is inversely proportional to the

weathering index CIA, with more aluminous, high CIA samples correlating with low CEC samples that have more simple clay minerals.

6. Conclusions

We present a recommended sediment leach protocol for an improved terrigenous signature extraction from marine sediments that includes a cation exchange wash. We find that ions having higher concentrations in seawater are predominantly displaced by the cation exchange wash, and conclude that the derived geochemical data represents a more accurate terrestrial signal. Therefore, this procedure is favourable for major and trace elements and leads to Nd and Sr isotope ratios that are more truly representative of the terrestrial detritus. The observed magnitude of change in the Sr and Nd isotopes between washed and non-washed aliquots is large. Nevertheless, whether the Cs^+ -treatment was used or not, the overall downcore trends and correlations between isotopes are similar, and hence whether or not it is applied, general climate reconstruction conclusions are likely to be similar.

Due to flocculation and rapid settling of clay minerals in Cs-washed samples, it is evident that a dried Cs-washed aliquot is more homogenous, and that $^{40}\text{K}/^{40}\text{Ar}$ age measured on it will be more reproducible and reflect the bulk age of the sediment.

For the accurate determination for the CEC of the clay fraction of marine sediment, we recommend adding to the procedure a step that oxidizes organic matter. This may be important, even if the concentration of organic matter in the sediment is low.

Because of the relationship between cation exchange capacity, clay mineralogy, soil flushing, and ultimately annual precipitation and climate conditions, CEC could, with further calibration efforts, be useful as a terrestrial chemical weathering proxy. However, CEC's potential in this capacity is difficult to tell due to the limited range of CEC (42–50 meq/100 g) in this study. A detailed survey of CEC of clay minerals in different depositional and climate settings would be necessary to relate the CEC of the clay mineral fraction to chemical weathering regimes.

Author contributions

M.H.S and C.L raised the funding for this pilot study. S.H. and S.G. contributed financially to the analysis cost and hosted M.H.S at LDEO where analyses were performed. S.H., M.H.S., and S.G. designed the initial idea for this pilot study. M.H.S. conducted much of the laboratory work for the sediment preparations, dissolution, and column chemistry. S.H. and D.B. conducted the major/trace element analysis for this study. D.B. helped with K/Ar age analysis, designed the K/Ar age settling study. X.H. performed the clay mineralogy analyses. M.Y.C. supervised M.H.S. during laboratory work and conducted together with M.H.S. the isotope measurements. T.L. analyzed samples for K/Ar ages. M.J. and A.H. helped with testing protocols for the Cs-wash step and its effect on K/Ar ages. M.H.S and D.B. structured the outline of the paper and wrote the manuscript. All authors read and contributed to the final manuscript.

Declaration of competing interest

The authors declare that they have no known competing financial interests or personal relationships that could have appeared to influence the work reported in this paper.

Acknowledgement

M.H.S. and C.L. acknowledge funding for this project from UK Natural Environment Research Council (NERC) IODP Moratorium grant: NE/N020286/1: "Pliocene palaeoclimate off SE Africa: Insights from IODP expedition 361." M.H.S. additionally received salary funding from the European Research Council under the European Community's

Seventh Framework Programme (FP7/2007-2013)/ERC grant agreement n° 61005. This work was partly supported by the Research Council of Norway, through its Centres of Excellence funding scheme, SFF Centre for Early Sapiens Behaviour (SapienCE), project number 262618. We thank the Captain, officers, crew and especially all scientists sailing on IODP expedition 361. We thank Charlotte Skonieczny for her input on clay minerals. We also thank Alison Corley and Louise Bolge at LDEO for help with laboratory and analytical work on sample material of core U1478. We thank Marcus Gutjahr and one anonymous reviewer for their time and thoughts on this manuscript.

Appendix A. Supplementary data

Supplementary data to this article can be found online at <https://doi.org/10.1016/j.chemgeo.2019.119449>.

References

- Abouchami, W., Galer, S.J.G., 1998. The provinciality of Pb isotopes in Pacific Fe-Mn deposits. *Mineral. Mag.* 62A, 1–2.
- Allègre, C.J., Dupré, B., Nègre, P., Gaillardet, J., 1996. Sr-Nd-Pb isotope systematics in Amazon and Congo River systems: constraints about erosion processes. *Chem. Geol.* 131 (1), 93–112.
- Angino, E.E., Billings, G.K., Andersen, N., 1966. Observed variations in the strontium concentration of sea water. *Chem. Geol.* 1, 145–153.
- Bache, B.W., 1976. The measurement of cation exchange capacity of soils. *J. Sci. Food Agr.* 27 (3), 273–280. <https://doi.org/10.1002/jsfa.2740270313>.
- Biscaye, P.E., 1965. Mineralogy and sedimentation of recent deep-sea clay in the Atlantic Ocean and adjacent seas and oceans. *GSA Bull.* 76 (7), 803–832.
- Bischoff, J.L., Menking, K.M., Fitts, J.P., Fitzpatrick, J.A., 1997. Climatic oscillations 10,000–155,000 yr B.P. at Owens Lake, California reflected in glacial rock flour abundance and lake salinity in core OL-92. *Quat. Res.* 48 (3), 313–325.
- Carroll, D., Starkey, H.C., 2013. Effect of sea-water on Clay Minerals 1 A2 - INGERSON, EARL. *Clay Clay Miner.* 80–101 Pergamon.
- Eglinton, B.M., Armstrong, R.A., 2004. The Kaapvaal Craton and adjacent orogens, southern Africa: a geochronological database and overview of the geological development of the craton. *S. Afr. J. Geol.* 107 (1–2), 13–32.
- Esquevin, J., 1969. Influence de la composition chimique des illites sur leur cristallinité. *Bulletin du Centre de Recherches de Pau-SNPA* 3, 147–153.
- Franzese, A.M., Hemming, S.R., Goldstein, S.L., Anderson, R.F., 2006. Reduced Agulhas Leakage during 3 Glacial Maximum inferred from an integrated provenance and flux study. *Earth Planet. Sci. Lett.* 250 (1–2), 72–88.
- Franzese, A.M., Hemming, S.R., Goldstein, S.L., 2009. Use of strontium isotopes in detrital sediments to constrain the glacial position of the Agulhas Retroflexion. *Paleoceanography* 24 (2), PA2217.
- Garzanti, E., Padoan, M., Setti, M., López-Galindo, A., Villa, I.M., 2014. Provenance versus weathering control on the composition of tropical river mud (southern Africa). *Chem. Geol.* 366, 61–74.
- Goldstein, S.L., O’Nions, R.K., 1981. Nd and Sr isotopic relationships in pelagic clays and ferromanganese deposits. *Nature* 292 (5821), 324–327.
- Goldstein, S.L., O’Nions, R.K., Hamilton, P.J., 1984. A Sm-Nd isotopic study of atmospheric dusts and particulates from major river systems. *Earth Planet. Sci. Lett.* 70 (2), 221–236.
- Gombiner, J.H., Hemming, S.R., Hendy, I.L., Bryce, J.G., Blichert-Toft, J., 2016. Isotopic and elemental evidence for Scabland Flood sediments offshore Vancouver Island. *Quat. Sci. Rev.* 139, 129–137.
- Gutjahr, M., et al., 2007. Reliable extraction of a Deepwater trace metal isotope signal from Fe-Mn oxyhydroxide coatings of marine sediments. *Chem. Geol.* 242 (3), 351–370.
- Hahn, A., et al., 2016. Holocene paleo-climatic record from the South African Namaqualand mudbelt: a source to sink approach. *Quat. Int.* 404, 121–135 Part B.
- Hall, I., Hemming, S., LeVay, L., Barker, S., Berke, M., Brentegani, L., Caley, T., Cartagena-Sierra, A., Charles, C., Coenen, J., Crespin, J., Franzese, A., Gruetzner, J., Han, X., Hines, S., Jimenez Espejo, F., Just, J., Koutsodendris, A., Kubota, K., N., L., Norris, R., Periera dos Santos, T., Robinson, R., Rolinson, J., Simon, M., Tanguan, D., van der Lubbe, J., Yamane, M., Zhang, H., 2017. Expedition 361 summary. In: *Proceedings of the International Ocean Discovery Program* 361.
- Houghton, P.D.W., Todd, S.P., Morton, A.C., 1991. Sedimentary provenance studies. *Geol. Soc. Lond., Spec. Publ.* 57 (1), 1–11.
- Hemming, S.R., et al., 2002. $^{40}\text{Ar}/^{39}\text{Ar}$ ages and $^{40}\text{Ar}^*$ concentrations of fine-grained sediment fractions from North Atlantic Heinrich layers. *Chem. Geol.* 182 (2), 583–603.
- Henderson, G.M., Martel, D.J., O’Nions, R.K., Shackleton, N.J., 1994. Evolution of sea-water $^{87}\text{Sr}/^{86}\text{Sr}$ over the last 400 ka: the absence of glacial/interglacial cycles. *Earth Planet. Sci. Lett.* 128 (3), 643–651.
- Imai, N., Terashima, S., Itoh, S., Ando, A., 1996. Compilation of analytical data on nine GSJ Geochemical reference samples “Sedimentary rock series” *Geostand. Newslett.* 20 (2), 165–216.
- Jacobsen, S.B., Wasserburg, G.J., 1980. Sm-Nd isotopic evolution of chondrites. *Earth Planet. Sci. Lett.* 50 (1), 139–155.
- Jelsma, H.A., Dirks, P.H.G.M., 2002. Neoproterozoic Tectonic Evolution of the Zimbabwe Craton. 199(1). Geological Society, London, Special Publications, pp. 183–211.
- Jiménez-Espinosa, R., Vázquez, M., Jiménez-Millán, J., 2007. Differential weathering of granitic stocks and landscape effects in a Mediterranean climate, Southern Iberian Massif (Spain). *Catena* 70 (2), 243–252.
- Jones, K., 2010. An Evaluation of Radiogenic Isotopes as Tracers of Ocean Circulation and Sediment Transport: Ocean Modeling, Seawater Analysis, and Sediment Studies. Columbia University, New York, US.
- Jung, S.J.A., Davies, G.R., Ganssen, G.M., Kroon, D., 2004. Stepwise Holocene aridification in NE Africa deduced from dust-borne radiogenic isotope records. *Earth Planet. Sci. Lett.* 221 (1–4), 27–37.
- Kreissig, K., F. Nägler, T., Kramers, J., van Reenen, D., Smit, C.A., 2000. An Isotopic and Geochemical Study of the Northern Kaapvaal Craton and the Southern Marginal Zone of the Limpopo Belt: Are they Juxtaposed Terranes? 50 (1–25 pp).
- Lamont, T., Roberts, M.J., Barlow, R.G., van den Berg, M.A., 2010. Circulation patterns in the Delagoa Bight, Mozambique, and the influence of deep ocean eddies. *Afr. J. Mar. Sci.* 32 (3), 553–562.
- Lutjeharms, J.R.E., 2006. Three decades of research on the greater Agulhas current. *Ocean Sci. Discuss.* 3 (4), 939–995.
- Milliman, J.D., Meade, R.H., 1983. World-Wide delivery of river sediment to the Oceans. *J. Geol.* 91 (1), 1–21.
- Morad, S., Ketzer, J.M., De Ros, L.F., 2000. Spatial and temporal distribution of diagenetic alterations in siliciclastic rocks: implications for mass transfer in sedimentary basins. *Sedimentology* 47 (s1), 95–120.
- Nesbitt, H.W., Young, G.M., 1982. Early Proterozoic climates and plate motions inferred from major element chemistry of lites. *Nature* 299, 715.
- Odin, G.S., 1976. La glauconite GL-O, étalon inter-laboratoires pour l’analyse radiochronométrique. *Analisis* 4, 287–291.
- Palmer, M.R., Elderfield, H., 1985. Sr isotope composition of sea water over the past 75 Myr. *Nature* 314, 526. <https://doi.org/10.1038/314526a0>.
- Reason, C.J.C., Jury, M.R., 1990. On the generation and propagation of the southern African coastal low. *Q. J. R. Meteorol. Soc.* 116 (495), 1133–1151.
- Reason, C.J.C., Landman, W., Tennant, W., 2006. Seasonal to decadal prediction of Southern African climate and its links with variability of the Atlantic Ocean. *Bull. Am. Meteorol. Soc.* 87 (7), 941–955.
- Rutberg, R.L., Goldstein, S.L., Hemming, S.R., Anderson, R.F., 2005. Sr isotope evidence for sources of terrigenous sediment in the Southeast Atlantic Ocean: is there increased available Fe for enhanced glacial productivity? *Paleoceanography* 20 (1), PA1018.
- Schaetzl, R.J., Thompson, M.L., 2015. *Soils: Genesis and Geomorphology: Second Edition*. Cambridge University Press, Cambridge, pp. 795.
- Schüürman, J., Hahn, A., Zabel, M., 2019. In search of sediment deposits from the Limpopo (Delagoa Bight, southern Africa): deciphering the catchment provenance of coastal sediments. *Sediment. Geol.* 380, 94–104.
- Shao, J., Yang, S., 2012. Does chemical index of alteration (CIA) reflect silicate weathering and monsoonal climate in the Changjiang River basin? *Chin. Sci. Bull.* 57 (10), 1178–1187.
- Tachikawa, K., Athias, V., Jeandel, C., 2003. Neodymium budget in the modern ocean and paleo-oceanographic implications. *J. Geophys. Res. Oceans* (C8), 108.
- Tanaka, T., et al., 2000. JNdi-1: a neodymium isotopic reference in consistency with LaJolla neodymium. *Chem. Geol.* 168 (3), 279–281.
- Tessier, A., Campbell, P.G.C., Bisson, M., 1979. Sequential extraction procedure for the speciation of particulate trace metals. *Anal. Chem.* 51 (7), 844–851.
- Tyson, P.D., Preston-Whyte, R.A., 2000. *The Weather and Climate of Southern Africa*. Oxford University Press, Cape Town.
- van de Flierdt, T., et al., 2016. Neodymium in the oceans: a global database, a regional comparison and implications for palaeoceanographic research. *Philos. Trans. R. Soc. A Math. Phys. Eng. Sci.* 374 (2081), 20150293.
- van der Lubbe, H.J.L., Frank, M., Tjallingii, R., Schneider, R.R., 2016. Neodymium isotope constraints on provenance, dispersal, and climate-driven supply of Zambezi sediments along the Mozambique margin during the past ~45,000 years. *Geochem. Geophys. Geosyst.* 17 (1), 181–198.
- Weis, D., et al., 2006. High-precision isotopic characterization of USGS reference materials by TIMS and MC-ICP-MS. *Geochem. Geophys. Geosyst.* 7 (8).
- Zabel, M., Bickert, T., Dittert, L., Haese, R.R., 1999. Significance of the sedimentary Al:Ti ratio as an indicator for variations in the circulation patterns of the equatorial North Atlantic. *Paleoceanography* 14 (6), 789–799.